J Fusion Energ (2016) 35:807–815
DOI 10.1007/s10894-016-0108-8

ORIGINAL RESEARCH

Effects of Power Terms and Thermodynamics on the Contraction of Pinch Radius in Plasma Focus Devices Using the Lee Model

M. Akel[1] · Sh. Ismael[1] · S. Lee[2,3,4] · S. H. Saw[2,5] · H. J. Kunze[6]

Published online: 20 July 2016

Abstract The influence of the power terms Joule heating and radiative losses on the pinch radius in plasma focus devices is studied. Numerical experiments were carried out using the Lee model on three plasma focus devices spanning a large range of storage energy (PF400, INTI PF, PF1000) with different filling gases (N, O, Ne, Ar, Kr, Xe). Six possible regimes each characterized by a combination of significant power terms affecting plasma focus dynamics are found and discussed. These six possible regimes are further moderated by thermodynamic effects related to the specific heat ratio SHR of the plasma. In PF1000, the thermodynamic compression effects are clearly apparent in the radius ratio versus pressure curve for nitrogen which with atomic number $Z_n = 7$ is less radiative than neon with $Z_n = 10$, the dominant line radiation being proportional to Z_n^4. In neon radiative compression at optimum pressure is so dominant that it masks thermodynamic compression in the compression versus pressure graph. Results show that plasma radiation losses enhance the contraction of the plasma focus pinch radius within suitable pressure ranges characteristic of each machine for each gas discussed in this paper. The radiation enhancement of compression increases with the atomic number of the gas.

Keywords Lee model · Pinch radius · Radiative powers · Radiative contraction · Different gases

✉ M. Akel
pscientific@aec.org.sy

[1] Department of Physics, Atomic Energy Commission, P.O. Box 6091, Damascus, Syria

[2] Institute for Plasma Focus Studies, 32 Oakpark Drive, Chadstone, VIC 3148, Australia

[3] University of Malaya, Kuala Lumpur, Malaysia

[4] INTI International University, 71800 Nilai, Malaysia

[5] Nilai University, 1, Persiaran Universiti, Putra Nilai, 71800 Nilai, Malaysia

[6] Institute for Experimental Physics V, Ruhr-University Bochum, Bochum, Germany

Introduction

The plasma focus has wide-ranging application potentials due to its intense radiation of soft X-ray, hard X-ray, electron and ion beams, and fusion neutrons [1] when operated in deuterium. The use of gases such as Ne, Ar, Kr and Xe for generation of specific SXR or EUV lines for micro-lithography applications [2–4] has been widely discussed in the literature as has the use of nitrogen and oxygen to generate the lines suitable for water-window microscopy [5]. Recently argon has been considered for micro-machining due to the harder characteristic line radiation [6]. Various gases including Kr have been discussed and used for fusion neutron yield enhancement due arguably to mechanisms such as thermodynamically enhanced pinch compressions. Information obtained from the Lee model [7, 8] includes axial and radial velocities and dynamics, dimensions and duration of the focus pinch, gross information of temperatures and densities within the pinch, soft X-ray emission characteristics and yield. Radiation-coupled dynamics was included in the gradually improved five-phase code leading to numerical experiments on radiation cooling. The vital role of a finite small disturbance speed discussed by Potter in a Z-pinch situation was incorporated together with real gas thermodynamics and radiation-yield terms. Plasma self-absorption was included in 2007 improving soft X-ray yield simulation in neon, argon and xenon among other gases [7, 8].

The Pease–Braginskii (P–B) current [9–12] is known to be that current flowing in a hydrogen pinch which is just large enough for the bremsstrahlung to balance Joule heating. It is known that in gases emitting strongly in line radiation, the radiation-cooled threshold current is considerably lowered. Lee et al. [9] showed that the equations of the Lee model code [8] may be used to compute this lowering. The code also shows the effect of radiation cooling when operated in the relevant regimes. It is suggested that the neutron enhancement effect of seeding could at least in part be due to the enhanced compression caused by radiation cooling [13]. Ali et al. [14] reported that the effect of self-absorption becomes significant when the plasma is dense enough to behave as optically thick. It is essential to account for the effect of self-absorption in that case. The effect of self-absorption of line radiation is investigated in argon plasma by observing the influence of pressure variation of the gas. On comparison of the results of numerical experiment considering both aspects, i.e. by including and excluding the self-absorption term in the Lee code, an obvious deviation between the trajectories is observed in the time interval 200–300 ns of the slow compression phase in a 3 kJ plasma focus. Results with self-absorption showed that the pinch undergoes slow and very gradual compression. Without self-absorption a much more severe compression occurred.

Recently, reduced Pease–Braginskii currents are estimated for a linear pinch in a range of gases namely D_2, He, Ne, Ar, Kr and Xe. A characteristic depletion time of the plasma focus pinch energy by radiation is defined which could be used as an indicator for expectation of radiative collapse. The depletion times in various gases are estimated in units of pinch duration. The values indicate that in D_2 and He, the radiation powers are small, resulting in such long depletion times that no radiative collapse may be expected in the lifetime of the focus pinch. In Ne, low tens of percent are radiated and significant cooling and reduction in the radius ratio may be anticipated. In Ar, Kr and Xe, the depletion time is only a fraction of the estimated pinch duration so radiative collapse may be expected. Numerical experiments are then carried out with a circuit-coupled code which incorporates radiation-coupled dynamics with plasma focus pinch-elongation and plasma self-absorption. The latter eventually limits the radiated power and stops the radiative collapse. These results show the detailed dynamics and confirm the expectations arising from depletion times discussed above [12]. Experimental studies of discharges in the plasma focus facility with neon filling and respective numerical simulations employing the radiative Lee code are also reported. The pinch currents exceed the Pease–Braginskii current, which indicates radiative losses start to be larger than Joule heating, and contraction of formed plasma should occur and was indeed observed. Crucial for the identification of such an effect were the parallel numerical simulations [15].

In this paper, the Lee Model is used in numerical experiments for different energy plasma focus devices with different gases to investigate the effects of pressure variations and the radiative powers on the pinch radius.

Theoretical Background

The Pease–Braginskii current is the value of current (1.6 MA) at which bremsstrahlung radiation (considered as a loss from the plasma) equals Joule heating of the plasma pinch column in hydrogen assuming Spitzer resistivity. When the pinch current exceeds this value, bremsstrahlung losses exceed Joule heating and the plasma pinch begins to experience radiative cooling effects at progressively higher currents, until in severe cases, radiative collapse may be observed. The P–B current only considers bremsstrahlung, since at the high temperatures experienced in the hydrogen or deuterium pinch, the gases are fully ionized and there is no line radiation. For gases such as neon, argon, krypton and xenon, there may still be line radiation even at the high pinch temperatures. This line radiation may considerably exceed the effect of bremsstrahlung which thus radiation cooling is enhanced and radiative collapse may occur at much lower currents. In other words for these heavier gases the 'Pease–Braginskii' or threshold current is much lower than the threshold (or P–B) current applied to hydrogen. However, the critical current is only one condition for the occurrence of radiative collapse. Another condition would be the magnitude of the excess radiative power dQ/dt acting to reduce the energy in the pinch [12].

We consider the following powers (all quantities are in SI units unless otherwise stated) respectively bremsstrahlung, recombination, line radiation and Joule heating, generated in a plasma column of radius r_p, length z_f at temperature T:

$$\text{Pbrem} = \frac{dQ_{brem}}{dt} = -1.6 \times 10^{-40} N_i^2 Z_{eff}^3 \left(\pi r_p^2\right) z_f T^{0.5} \quad (1)$$

$$\text{Prec} = \frac{dQ_{rec}}{dt} = -5.92 \times 10^{-35} N_i^2 Z_{eff}^5 \left(\pi r_p^2\right) z_f / T^{0.5} \quad (2)$$

$$\text{Pline} = \frac{dQ_{line}}{dt} = -4.6 \times 10^{-31} N_i^2 Z_{eff} Z_n^4 \left(\pi r_p^2\right) z_f / T \quad (3)$$

$$\text{PJ} = \frac{dQ_J}{dt} = 1300 \cdot \frac{Z_{eff} \cdot z_f}{\pi r_p^2} \cdot I^2 \cdot T^{-\frac{3}{2}} \quad (4)$$

where number density N_i, effective charge number Z_{eff}, atomic number of gas Z_n, pinch radius r_p, pinch length z_f, plasma temperature T and circuit current I. The radiation

power may not completely leave the plasma depending on the plasma self-absorption which depends primarily on temperature and integrated density of the plasma column. Any plasma self-absorption of the radiation reduces the amount of radiation loss calculated from Eqs. 1–3.

The code uses the following equation for the radiation-coupled piston position r_p [7, 8] derived from the first law of thermodynamics:

$$\frac{dr_p}{dt} = \frac{-\frac{r_p}{\gamma I}\frac{dI}{dt} - \frac{1}{\gamma+1}\frac{r_p}{z_f}\frac{dz_f}{dt} + \frac{4\pi(\gamma-1)}{\mu\gamma z_f}\frac{r_p}{f_c^2 I^2}\frac{dQ}{dt}}{\frac{\gamma-1}{\gamma}} \quad (5)$$

where I is the total discharge current in the circuit, f_c is the fraction of current flowing into the pinch, z_f is the length of the pinch, and γ is the specific heat ratio SHR of the plasma. dQ/dt (or Qdot) is the total power term, which includes Joule heating PJ (which is a power gain term) and radiative loss PRAD (PRAD = Pbrem + Prec + Pline) after modified by plasma self-absorption. When the total power is negative, energy is lost from the plasma adding a negative component to dr_p/dt which tends to reduce the radius r_p. This causes radiatively enhanced compression which escalates to radiative collapse when the effect is severe.

We carry out numerical experiments with the Lee code into which a plasma self-absorption effect is incorporated following Khattak [16] with a smoothened transition from opacity-corrected volume emission to surface emission when opacity effects exceed a set limit.

Four Scenarios of Power Terms

The code models all these effects and properties in a coupled fashion. In this work, for studying the effect of the radiative powers on the pinch plasma radius, we carried out numerical experiments using the Lee model with the following four scenarios for the total power Qdot:

S1: With the total power Qdot = PJ + PRAD.
S2: Without Joule heating and radiative losses Qdot = 0.
S3: With the Joule heating effect only Qdot = PJ.
S4: With radiative losses only Qdot = PRAD.

Of the four scenarios S1 is the one including all the terms of Qdot and it is the scenario modelled in the code. The other three scenarios S2–S4 hypothetically omit one or the other of Joule heating and radiative loss terms, or both.

For each device operated with different gas filling the radius ratio (r_p/a) is plotted versus the operating pressure for each scenario S1 to S4.

Six Regimes Defined by the Order of Values Calculated with the Four Scenarios

These four graphs are placed on the same chart and there are six possible combinations (regimes) distinguishable by the order of the magnitude of values calculated with the four scenarios.

The six regimes are:

R1. Both PJ and PRAD significant (mod PJ > mod PRAD): order of values: S3 highest, then S1, then S2, then S4 lowest.
R2. Both PJ and PRAD significant (mod PJ < mod PRAD): order of values: S3 highest, then S2, then S1, then S4 lowest.
R3. Both PJ and PRAD significant (mod PJ = mod PRAD): order of values: S3 highest, then S2 = S1 (or very close together), then S4 lowest.
R4. PJ significant and PRAD insignificant: order of values: S3 = S1 (or very close together) these being higher than S2 = S4 (or S2 slightly greater than S4).
R5. PJ insignificant and PRAD significant: order of values: S3 = S2 (or S3 slightly greater than S2) these being higher, then S1 = S4 (or these values being very close to each other).
R6. Both PJ and PRAD insignificant: order of values: S1 = S2 = S3 = S4 (all 4 values being the same).

Thus by looking at the relative positions of the 4 radius ratios (r_p/a) versus operating pressure curves plotted from S1 to S4, not only can we obtain information of the pressures at which radiative cooling and collapse occur, but we can differentiate further the six regimes of operation across the pressure range.

Numerical Experiments: Results and Discussion

The configurations (tube and electrical parameters) of the three devices are collated in Table 1.

To start the numerical experiments we configure the Lee model code to operate as one of the above plasma focus devices. We then fit the computed current trace to a measured current trace of that device [20], obtaining the appropriate set of model parameters f_m, f_c, f_{mr}, f_{cr} for the particular plasma focus (see Table 2). These fitted values of the model parameters are then used for the particular device for computation of all the discharges at various pressures for each of the scenarios S1 to S4.

Results are presented for each gas in Figs. 1, 2, 3, 4, 5 and 6, respectively. Note that the curve S1, which includes all effects with Qdot = PJ + PRAD, shows the correct result of the code. The other three curves illustrate when

Table 1 Tube and electrical parameters for various plasma focus devices

Device (Ref.)	E (kJ)	a (cm)	b (cm)	Z_0 (cm)	L_0 (nH)	C_0 (μF)	I_{peak} (kA)	V_0 (kV)
PF400 [17]	0.4	0.6	1.55	2.8	38	0.88	130	28
INTI PF [18]	3.4	0.95	3.2	16	110	30	195	15
PF1000 [19]	353	11.55	16	60	33	1332	2500	23

Table 2 Parameters of interested plasma focus devices

Device (Ref.)	L_0 (nH)	C_0 (μF)	R_0 (mΩ)	V_0 (kV)	f_m	f_c	f_{mr}	f_{cr}
PF400 [17]	40	0.95	10	28	0.08	0.7	0.11	0.7
INTI PF [18]	110	30	12	15	0.06	0.7	0.16	0.7
PF1000 [19]	33	1332	3	23	0.1	0.7	0.25	0.7

L_0, C_0, r_0, inductance, capacitance, and resistance of the capacitor bank, respectively; V_0, tube voltage, axial phase; f_m, mass swept up factor; f_c, plasma current factor, radial phase; f_{mr}, mass swept up factor; f_{cr}, plasma current factor

one or the other or both of the power terms are hypothetically removed.

Nitrogen Plasma Focus

Figure 1 presents our results in nitrogen. The radius ratios (r_p/a) are plotted for each machine at various pressures for each of the four scenarios S1–S4. Figure 1a is for PF400, 1b for INTI PF and 1c for PF1000.

Figure 1a shows that the PF400 is in regime R6 at low pressure, then above 0.5 Torr the regime changes and becomes R4. While for INTI PF (Fig. 1b) at low pressure is R6, above 0.7 Torr becomes R4, above 1.5 Torr becomes R1, and then above 3 Torr becomes again R4. In PF1000 (Fig. 1c) the situation is more complicated: it starts at the lowest pressure regime R6 (both terms insignificant), then becomes R5 (strongly radiative), then at 0.7 Torr becomes R2 (radiative but Joule heating also becoming significant), then at 1.7 Torr becomes R1 (radiative but Joule term starting to dominate), then at 2.6 Torr becomes R4 (Joule term dominates) and above 4 Torr becomes R6 (both terms insignificant).

Effect of Thermodynamics, the Specific Heat Ratio

At this point we note in Fig. 1a that the lowest radius ratio in the R5 (strongly radiative) regime occurs at around 1 Torr with a value of 0.138 and yet at higher pressures during the R4 (Joule term dominates) regime the radius ratio has a minimum value of less than 0.13 at 5 Torr. This seems contradictory since the strong radiation should reduce the radius ratio whilst the Joule heating should increase the radius ratio. There must thus be another mechanism which we have not accounted for in our analysis thus far. The explanation is in Eq. (5). So far we have discussed the effect of dQ/dt in terms of its components, radiation and Joule heating. The other effect is the specific heat ratio SHR γ. In the plasma focus pinch at low pressures in a gas like nitrogen the plasma is fully ionized and the value of γ moves up towards 5/3, i.e. to that of a perfect gas. As pressure is increased the plasma moves towards freely ionizing in which state its value of γ goes as low as 1.2. The net effect is that at high pressures the right hand most term (involving dQ/dt) in the numerator in Eq. 5 is reduced in magnitude by a factor as much as 3 due to the change in γ, whilst the other two terms (dynamic power) in the numerator are relatively unchanged. Thus the thermodynamic effect (due to SHR) can reduce the effect of the dQ/dt terms relative to the dynamic power terms.

This is the situation where the enhanced thermodynamic compression at high pressures dominates (masks) the effect of dQ/dt in the case of nitrogen ($Z_n = 7$). The situation of a much more strongly radiating gas like neon ($Z_n = 10$) is somewhat different and will be discussed in the appropriate section.

Oxygen Plasma Focus

The radius ratio were plotted at various oxygen pressures for each of four Qdot cases.

The following Fig. 2a–c show variations of radius ratio versus pressures on PF400, INTI PF and PF1000 operated with oxygen, respectively, for Qdot cases.

Figure 2a shows that the PF400 operated at low pressure has regime 6, then above 0.7 Torr becomes regime 4, then with higher pressures above 2.3 Torr becomes regime 1, and finally above 3.5 Torr becomes regime 4. The INTI PF (Fig. 2b) at low pressure has regime 6, above 0.7 Torr becomes regime 4, above 1.3 Torr becomes regime 1, above 2.5 Torr becomes regime 4. While for PF1000 (Fig. 2c) starts at lowest pressure regime 6 (both terms insignificant) then becomes regime 5 (strongly radiative),

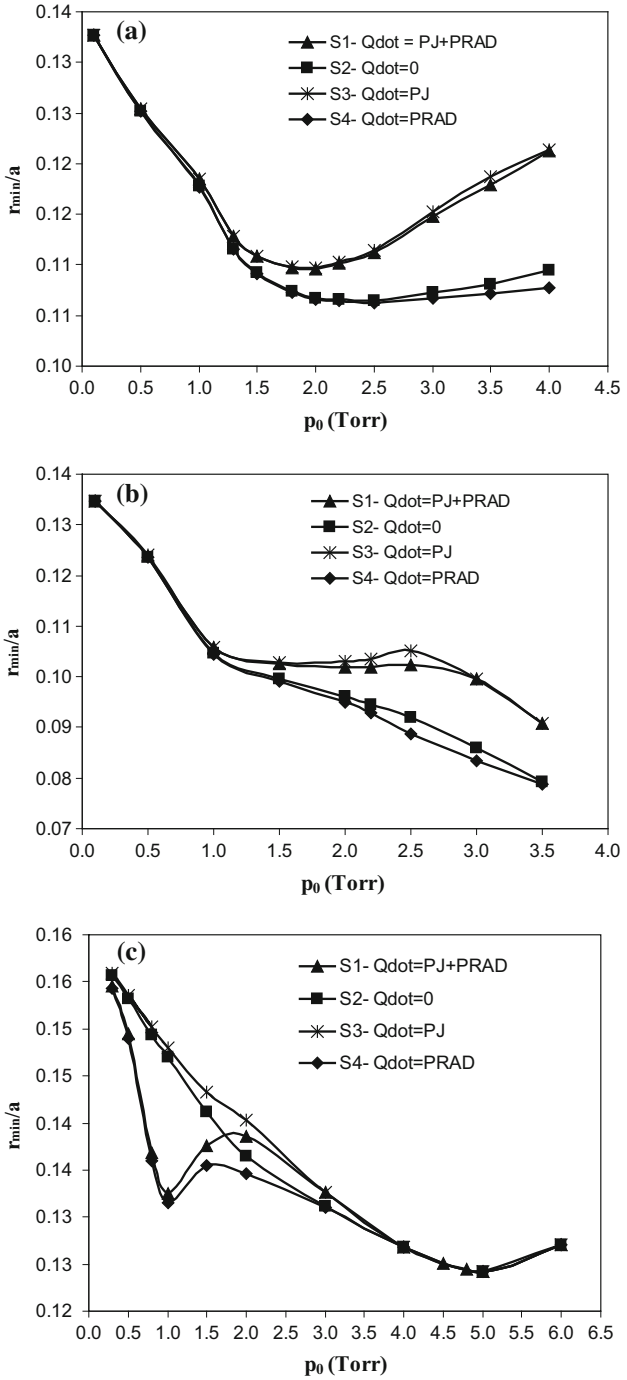

Fig. 1 Radius ratio (r_p/a) versus operating pressure for PF400 (**a**), INTI PF (**b**) and PF1000 (**c**) for nitrogen operation

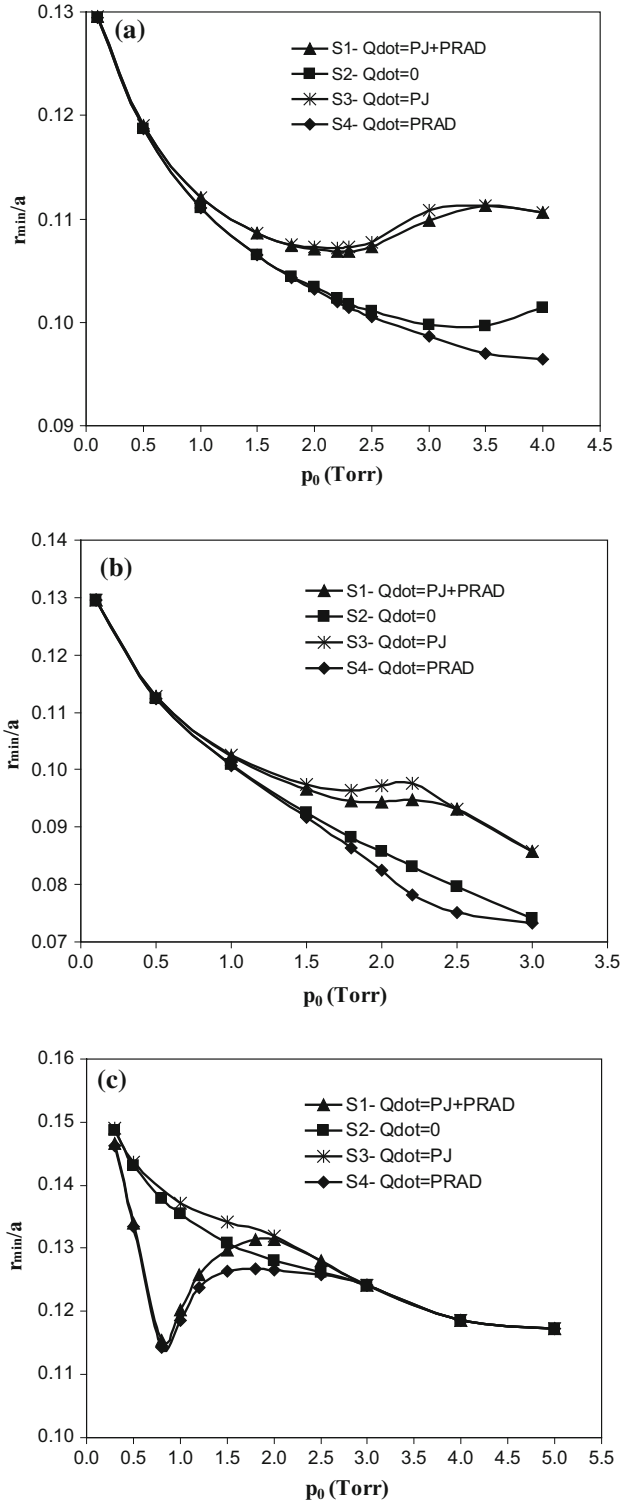

Fig. 2 Variations of radius ratio versus pressures on PF400 (**a**), INTI PF (**b**) and PF1000 (**c**) for oxygen plasma focus

then at 0.8 Torr becomes regime 2 (radiative but joule heating also becoming significant), then at 1.6 Torr becomes regime 1 (radiative but joule term starting to dominate), then at 2 Torr becomes regime 4 (joule term dominates) and above 3 Torr becomes regime 6 (both terms insignificant).

Neon Plasma Focus

The radius ratio were plotted at various neon pressures for each of four Qdot cases.

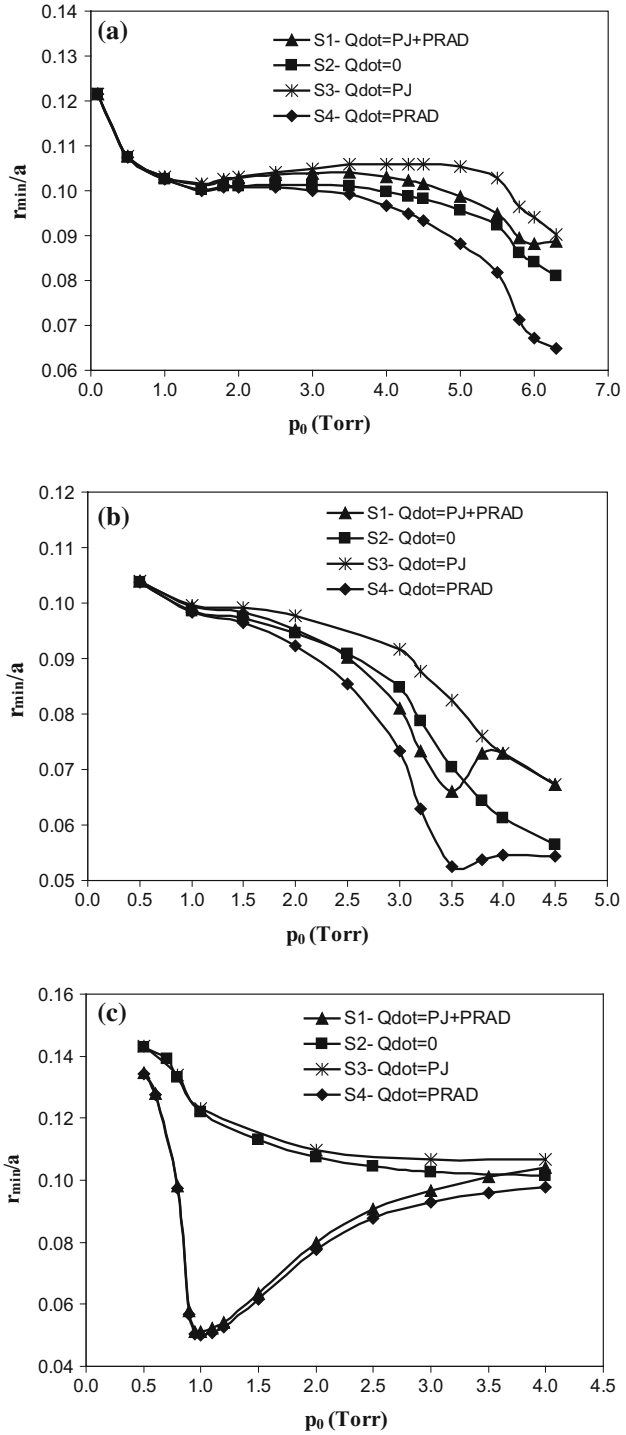

Fig. 3 Variations of radius ratio versus pressures on PF400 (**a**), INTI PF (**b**) and PF1000 (**c**) for neon plasma focus

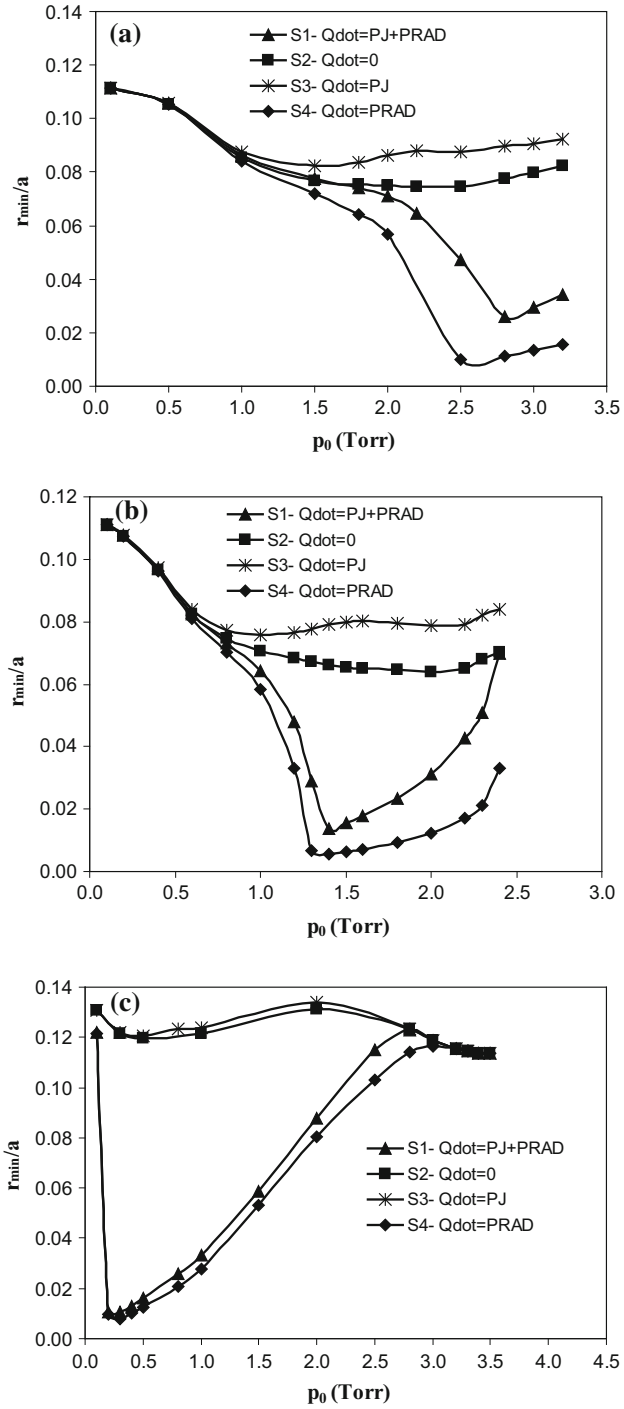

Fig. 4 Variations of radius ratio versus pressures on PF400 (**a**), INTI PF (**b**) and PF1000 (**c**) for argon plasma focus

The following Fig. 3a–c show variations of radius ratio versus pressures on PF400, INTI PF and PF1000 operated with neon, respectively, for Qdot cases.

Figure 3a shows that the PF400 at low pressure is in the regime 6, then above 1 Torr becomes in the regime 4, and above 2.5 Torr becomes regime 1. But INTI PF (Fig. 3b) has regime 6 at low pressure, above 0.7 Torr becomes regime 4, above 1.5 Torr becomes regime 3, above 2.5 Torr becomes regime 2, above 3.5 Torr becomes regime 1, above 4 Torr becomes regime 4. While the PF1000 (Fig. 3c) starts at lowest pressure with regime 5

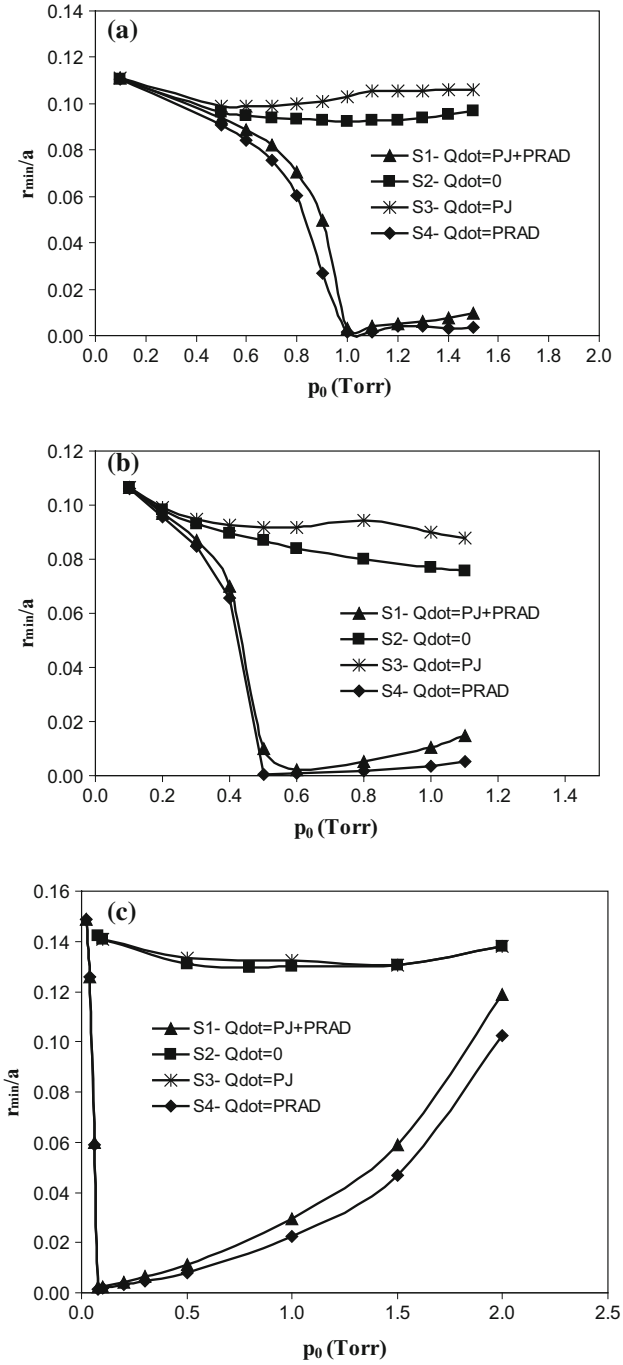

Fig. 5 Variations of radius ratio versus pressures on PF400 (**a**), INTI PF (**b**) and PF1000 (**c**) for krypton plasma focus

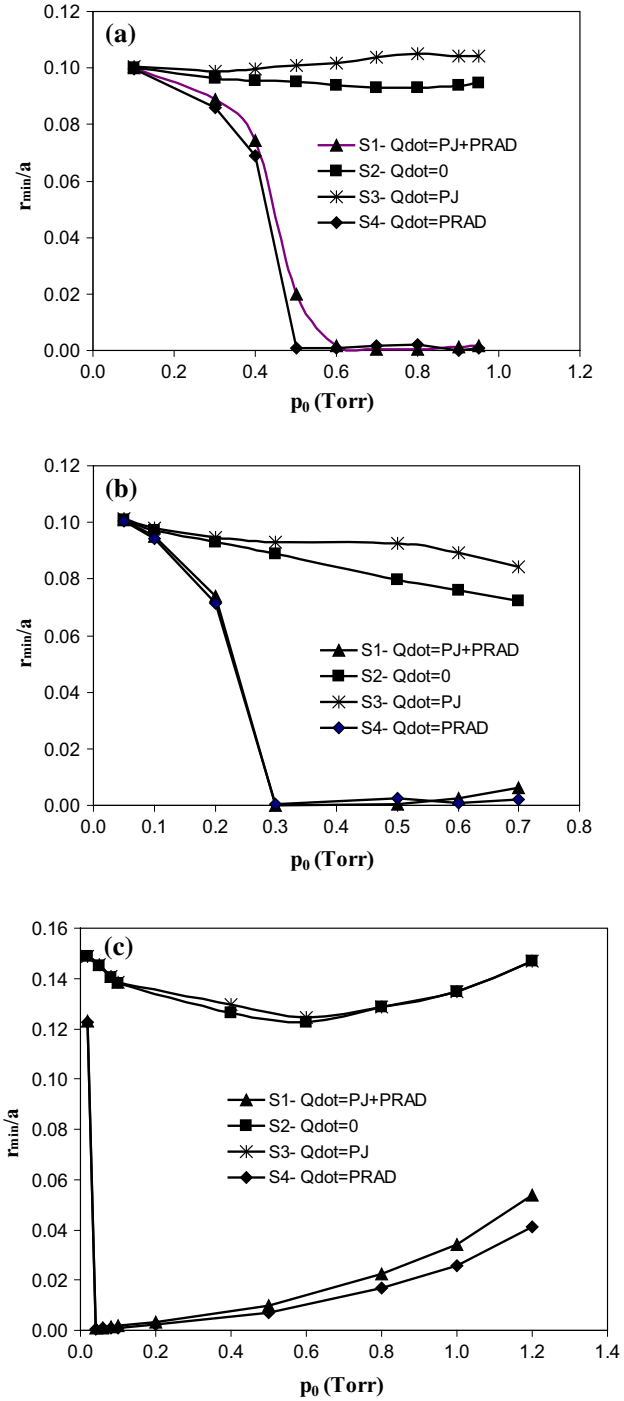

Fig. 6 Variations of radius ratio versus pressures on PF400 (**a**), INTI PF (**b**) and PF1000 (**c**) for xenon plasma focus

(strongly radiative), then at 1.2 Torr becomes regime 2 (radiative but joule heating also becoming significant), and above 3.5 Torr becomes regime 6 (both terms insignificant). We note in Fig. 3c that the thermodynamic masking effect discussed earlier for the case of PF1000 in nitrogen is not apparent in the case of neon because neon is much more strongly radiating than nitrogen (refer Eq. 3 which shows that the line radiation is proportional to atomic number to power 4). The radiative compression in R5 regime is so great that in comparison the thermodynamic compression is much less apparent.

Argon Plasma Focus

The radius ratios were plotted at various argon pressures for each of four Qdot cases.

The following Fig. 4a–c show variations of radius ratio versus pressures on PF400, INTI PF and PF1000 operated with argon, respectively, for Qdot cases.

Figure 4a shows that the PF400 at low pressure is in the regime 6, then above 1 Torr it moves into in the regime 3, and above 1.8 Torr finally becomes regime 2. INTI PF (Fig. 4b) has regime 6 at low pressure, above 0.6 Torr becomes regime 2, above 1.2 Torr becomes regime 5 (strongly radiative), and above 2.3 Torr becomes regime 3. While the PF1000 (Fig. 4c) starts at lowest pressure with regime 5 (strongly radiative), then at 0.4 Torr becomes regime 2 (radiative but joule heating also becoming significant), and above 2.8 Torr becomes regime 6 (both terms insignificant).

Krypton Plasma Focus

The radius ratios were plotted at various krypton pressures for each of the four Qdot cases.

Figure 5a–c show the variations versus pressure on PF400, INTI PF and PF1000 operated with krypton, respectively, for Qdot cases.

Figure 5a shows that the PF400 device at low pressure is in the regime 6, then above 0.5 Torr becomes in the regime 2, and above 1 Torr becomes regime 5 (strongly radiative). INTI PF (Fig. 5b) has regime 6 at low pressure, above 0.2 Torr becomes regime 2, above 0.3 Torr becomes regime 5 (strongly radiative), above 1 Torr becomes regime 2. While the PF1000 (Fig. 5c) starts at lowest pressure in regime 6 (both terms insignificant) then becomes regime 5 (strongly radiative), then at 0.4 Torr becomes regime 2 (radiative but joule heating also becoming significant), and above 2 Torr becomes regime 6 (both terms insignificant).

Xenon Plasma Focus

The radius ratios were plotted at various xenon pressures for each of the four Qdot cases.

Figure 6a–c show the variations of the radius ratio versus pressures on PF400, INTI PF and PF1000 operated with xenon, respectively, for Qdot cases.

Figure 6a shows that the PF400 at low pressure is in the regime 6, then above 0.1 Torr changes into regime 2, and above 0.5 Torr it becomes regime 5 (strongly radiative). INTI PF (Fig. 6b) has regime 6 at low pressure, above 0.1 Torr becomes regime 2, above 0.2 Torr becomes regime 5 (strongly radiative), and above 0.6 Torr becomes regime 2. While the PF1000 (Fig. 6c) starts at lowest pressure with regime 5 (strongly radiative), which remains dominant.

Radiative collapse phenomena have been also observed at higher pressure with heavy noble gases. From numerical experiments with nitrogen, oxygen, and neon plasma focus, it can be said that the radiative collapse phenomenon has been noticed but not as strong as for heavier gases. Finally, based on obtained results by five phase Lee model, we can say that the tube and electrical parameters, gas type and pressure of the plasma focus play an important role in radiative contraction/collapse creation. This phenomenon produces an extreme increase in tube voltage and generates huge line radiations in the plasma focus.

Conclusions

The Lee model code was run for different plasma focus devices (PF400, INTI PF, PF1000) with various gases like N, O, Ne, Ar, Kr and Xe and demonstrates radiative cooling leading to radiative contraction. Six possible regimes each characterized by a combination of significant power terms affecting plasma focus dynamics are found and discussed. These six possible regimes are further modified by thermodynamic effects related to the specific heat ratio SHR of the plasma. For gases with atomic number of 10 and above, intense line radiation from plasma foci has been found in a range of pressures, leading to a minimal value of the pinch radius. Comparing the radius ratio versus pressure curves in each gas of the three devices, it is noticed that the operational, geometrical and electrical parameters of the setup have an important role in determining the degree of radiative contraction and the operational regimes. The creation of the consequential extreme conditions of density and pulsed power is of interest for research and applications.

Acknowledgments M. Akel and Sh. Ismael would like to thank Director General of AECS, for encouragement and permanent support.

References

1. A. Bernard, H. Bruzzone, P. Choi, H. Chuaqui, V. Gribkov, J. Herrera, K. Hirano, A. Krejci, S. Lee, C. Luo, F. Mezzetti, M. Sadowski, H. Schmidt, K. Ware, C.S. Wong, V. Zoita, Scientific status of plasma focus research. Mosc. J. Phys. Soc. **8**, 93–170 (1998)
2. R.R. Prasad, M. Krishnan, Neon dense plasma focus point X-ray source for <0.25 μm lithography. SPIE **2194**, 120–128 (1994)
3. S. Lee, P. Lee, G. Zhang, X. Feng, V.A. Gribkov, M. Liu, A. Serban, T. Wong, IEEE Trans. Plasma Sci. **26**(4), 1119–1126 (1998)
4. K. Bergmann, O. Rosier, W. Neff, R. Lebert, Appl. Opt. **39**(22), 3833–3837 (2000)

5. R. Lebert, W. Neff, D. Rothweiler, J. X-Ray Sci. Technol. **6**, 2 (1996)
6. V.A. Gribkov, A. Srivastava, P.L.C. Keat, V. Kudryashov, Sing Lee. IEEE Trans. Plasma Sci. **30**, 1331–1338 (2002)
7. S. Lee, http://www.plasmafocus.net (2016)
8. S. Lee, J. Fusion Energ. **33**(4), 319–335 (2014)
9. S. Lee, S.H. Saw, J. Ali, Numerical experiments on radiative cooling and collapse in plasma focus operated in krypton. J. Fusion Energ. **32**, 42–49 (2013)
10. M. Akel, S. Lee, Radiative collapse in plasma focus operated with heavy noble gases. J. Fusion Energ. **32**(1), 111–116 (2013)
11. M. Akel, S. Lee, S.H. Saw, Numerical experiments in plasma focus operated in various gases. IEEE Trans. Plasma Sci. **40**(12), 3290–3297 (2012). doi:10.1109/TPS.2012.2220863
12. S. Lee, S.H. Saw, M. Akel, J. Ali, H.-J. Kunze, P. Kubes, M. Paduch, Conditions for radiative cooling and collapse in the plasma focus illustrated with numerical experiments on PF1000. IEEE Trans. Plasma Sci. **44**(2), 165–173 (2016). doi:10.1109/TPS.2015.2497269
13. S. Lee, S.H. Saw, Multi-radiation modelling of the plasma focus. in 5th *International Conference on Fronties of Plasma Physics and Technology*, 18–22 April 2011, Singapore
14. Z. Ali, S. Lee, F.D. Ismail, Saktioto, J. Ali, P.P. Yupapin, Phys. Proc. **8**, 393–400 (2011)
15. M. Akel, J. Cikhardt, P. Kubes, H.-J. Kunze, S. Lee, M. Paduch, S.H. Saw, Nukleonika **61**(2), 145–148 (2016)
16. N.A.D. Khattak, Anomalous Heating (LHDI). http://www.plasmafocus.net/IPFS/modelpackage/File3Appendix.pdf (2011)
17. L. Soto, C. Pavez, J. Moreno, M.J. Inestrosa-Izurieta, F. Veloso, G. Gutierrez, J. Vergara, A. Clausse, H. Bruzzone, F. Castillo, L.F. Delgado-Aparicio, Phys. Plasmas **21**, 122703 (2014)
18. S. Lee, T.Y. Tou, S.P. Moo, M. AEissa, A.V. Gholap, K.H. Kwek, S. Mulyodrono, A.J. Smith, Suryadi, W. Usada, M. Zakaullah, Am. J. Phys. **56**, 62 (1988)
19. V.A. Gribkov, A. Banaszak, B. Bienkowska, A.V. Dubrovsky, I. Ivanova-Stanik, L. Jakubowski, L. Karpinski, R.A. Miklaszewski, M. Paduch, M.J. Sadowski, M. Scholz, A. Szydlowski, K. TomaszewskiJ, J. Phys. D Appl. Phys. **40**, 3592–3607 (2007)
20. Sh Al-Hawat, M. Akel, S. Lee, S.H. Saw, J. Fusion Energ. **31**(1), 3–20 (2012)